Journal of Alloys and Compounds 505 (2010) 151–156

Contents lists available at ScienceDirect

Journal of Alloys and Compounds

journal homepage: www.elsevier.com/locate/jallcom

Nickel–boron electrochemical properties investigations

A.-F. Kanta[a,*], M. Poelman[b], V. Vitry[c], F. Delaunois[c]

[a] Service de Science des Matériaux, Université de Mons, 56 rue de l'Epargne, 7000 Mons, Belgium
[b] Materia Nova a.s.b.l, 56 rue de l'Epargne, 7000 Mons, Belgium
[c] Service de Métallurgie, Université de Mons, 56 rue de l'Epargne, 7000 Mons, Belgium

ARTICLE INFO

Article history:
Received 16 April 2010
Received in revised form 28 May 2010
Accepted 31 May 2010
Available online 11 June 2010

Keywords:
Nickel–boron
Electroless
Wear
Corrosion

ABSTRACT

Electroless nickel–boron (Ni–B) was synthesized on mild steel. Coating thickness was approximately 30 μm. Some of the coatings were submitted to a hardening heat treatment at 400 °C for 1 h in an atmosphere containing 95% Ar and 5% H_2 to improve their mechanical performance.

Heat treated and untreated samples were submitted to the Taber abrasion test to assess their wear resistance. The wear track was then examined by SEM and roughness measurement. The Taber Wear Index of untreated samples was slightly better than that of steel but heat treated samples attained TWI as small as 13.

The corrosion resistance of the Ni–B coatings was investigated by potentiodynamic polarization and electrochemical impedance spectroscopy. The EIS results showed diffusion phenomena in 0.1 M NaCl solution. Electroless Ni–B coating increases the corrosion resistance of steel and heat treatments allow a further enhancement. Wear decreases that resistance but the worn product keeps a better behaviour than uncoated parts.

1. Introduction

Electroless deposition processes experienced numerous modifications to meet the challenging needs of a variety of industrial applications [1]. The electroless nickel coatings may provide a possible solution for the low-cost hard surface layers, operating under adverse working conditions. Electroless nickel–boron plating is a chemical reduction process which depends upon the catalytic reduction of nickel ions in aqueous solution and the subsequent deposition of nickel metal without the use of electrical energy [2,3]. The coating may be surface-finished although the inherent geometric uniformity of the coating allows the coating to be used, in many cases, without further surface finishing.

It has been applied successfully in chemical, mechanical and electronic industries due to their desirable physical, mechanical properties and uniformity in thickness [4]. The corrosion resistance of coatings depends on the physicochemical properties of the coating such as the adherence, hardness and roughness of the substrate mainly. Recently, much attention is being paid towards borohydride-reduced electroless nickel plating. The properties of sodium borohydride-reduced electroless nickel coatings are often superior to those of deposits reduced with sodium hypophosphite [1]. The principal advantages of borohydride-reduced electroless nickel deposits are its hardness and superior wear resistance in the as-deposited condition [5]. Electroless Ni–B coatings are more wear resistant than tool steel and hard chromium coatings [1]. The major limitation of Ni–B coating is its relatively poor corrosion resistance compared to electroless Ni–P deposits. The difference in corrosion resistance between Ni–P and Ni–B coatings is due to the difference in their structure. Since borohydride-reduced electroless nickel deposit is not totally amorphous, the passivation films that form on its surface are not as glassy or protective as those that form on high-phosphorous coatings.

The corrosion behaviour of Ni–B deposits has not been extensively studied, thus only limited information is available for Ni–B deposits. Similarly to nickel–phosphorus, the corrosion behaviour of nickel–boron deposit can be dependent on many parameters such as its B content [6–8], the homogeneity of element distribution in the coating surface [6] and throughout the deposit, the surface morphology of the deposit (i.e. whether it is smooth, nodular, or possesses a cauliflower-like morphology) [9], the microstructure of the deposit (i.e. whether it is crystalline, amorphous, or composed of mixed phases) [10], the presence of impurity inclusions and their distribution in the deposit (e.g., Pb or S inclusions) [6,11], the nature of the substrate under the deposit, etc.

The present work intends to deposit Ni–B on steel substrates and to evaluate its microhardness, roughness, wear resistance and corrosion properties. The effect of heat treatment was studied. The surface morphologies following heat treatment, wear and corrosion testing were studied by scanning electron microscopy (SEM).

* Corresponding author. Tel.: +32 65 37 44 47; fax: +32 65 37 44 16.
E-mail address: abdoul.kanta@umons.ac.be (A.-F. Kanta).

0925-8388/$ – see front matter © 2010 Elsevier B.V. All rights reserved.
doi:10.1016/j.jallcom.2010.05.168

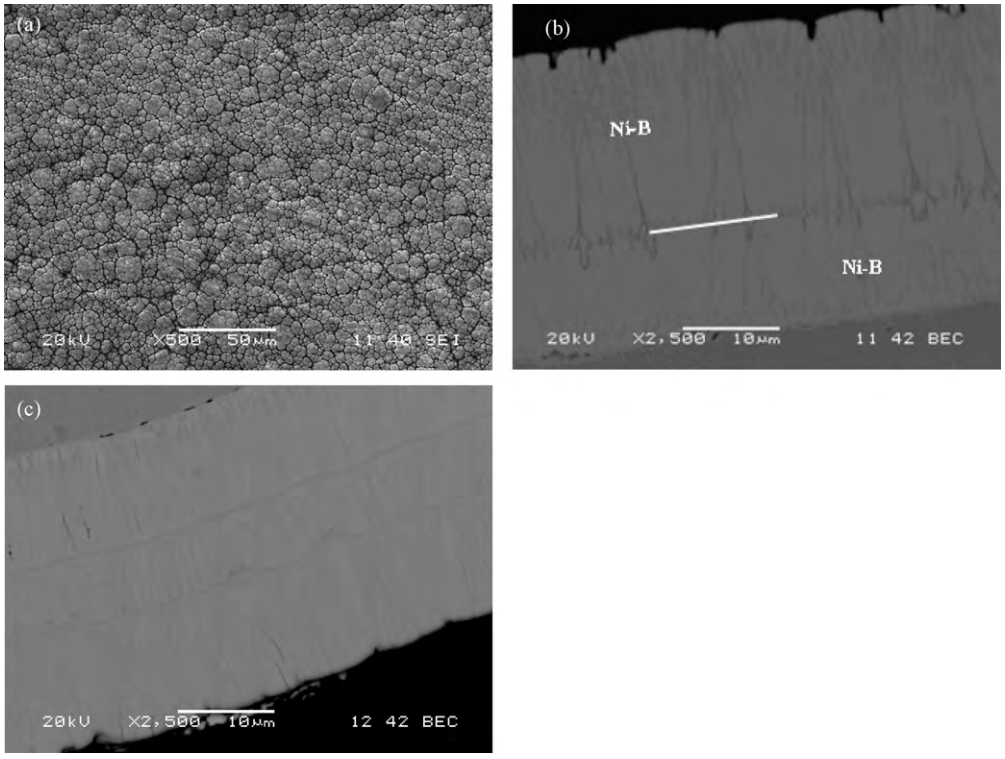

Fig. 1. SEM of Ni–B coating with replenishment: (a) surface morphology; (b) cross section morphology; (c) heat treated coating.

2. Experimental setups

2.1. Plating

ST 37 mild steel substrates (disc coupons with 10 cm diameter, 1 mm thick) were used for the deposition of Ni–B films. Before coating, the samples were mechanically cleaned. Subsequently, they were first manually ground on 1200 and 4000 grade SiC paper successively, degreased with acetone, rinsed in distilled water and air-dried. The sample surface was finally activated with a solution of HCl (30 vol.%) for 1 min, rinsed in distilled water and immersed in the deposition bath.

After the different pre-treatments the samples were put into the bath which is based on nickel chloride ($NiCl_2{\cdot}6H_2O$), sodium borohydride ethylene diamine and sodium hydroxide and small amounts of lead tungstate. This bath composition was described in detail elsewhere [3]. The volume of the bath was 8 dm^3. The plating solution was agitated.

To realize deposits with important thickness, the experiment was conducted without interruption for 90 min with an addition of reactive after the first 30 min (i.e. bath replenishment). The coatings obtained have average boron content close to 6 wt.% [12]. The coating thickness was calculated from the weight gain.

Some samples were subsequently heat treated at 400 °C for 1 h under a controlled atmosphere containing 95% Ar and 5% H_2. This is a standard treatment for the enhancement of the mechanical properties of electroless nickel–boron coatings [13].

2.2. Characterization methods

X-ray diffraction (XRD), using a Siemens D500 X-rays θ-θ apparatus applying Cu Kα, was employed to analyze the crystal structure of the coated film.

The abrasion resistance of the coatings was determined using Taber 5155 (Taber Industries, North Tonawanda, NY) apparatus. During this test, the coated sample is submitted to a steady speed rotation, under a weight inflicted by two wheels of hard material embedded in rubber which are rotating in the opposite direction. The test was carried out using CS17 abrasive rubber wheels, with a weight of 1000 g and a rotation speed of 70 rpm.

Philips XL 20 scanning electron microscopy (SEM) apparatus was used to characterize the structure and morphology of the coatings.

Roughness measurements were carried out using a Zeiss 119 Surfcom 1400D-3DF apparatus.

Microhardness measurements were carried out by Vickers technical. It was carried out in the growth direction of the coating and any damage occurring during this test will remain unseen because it will take place inside the coating.

The electrochemical properties were investigated using a Parstat 2273 potentiostat (including a frequency response analyzer, FRA). For all measurements, the coatings were masked with silicone so that only a 1 cm^2 area was exposed to the electrolyte. The electrochemical experiments were measured in 0.1 M NaCl aerated solution, at room temperature with a conventional three-electrode cell. The working electrode consists of the coated specimen, a platinum grid was used as a counter electrode and an Ag, AgCl/KCl (saturated) electrode as a reference electrode.

The anodic polarization curves were measured by a dynamic potential scanning technique. The electrode potential was raised from −250 to +600 mV/OCP at the rate of 10 mV min^{-1}. This large interval of scanning permits to detect if there are passivation phenomena.

EIS measurements were carried out in the frequency range 10^5–10^{-2} Hz, with a sinusoidal signal perturbation of 5 mV (root mean square). In order to minimize external interference, the electrochemical cell was placed in a Faraday cage.

3. Results and discussions

3.1. Morphology and composition of the coatings

Deposition of the coating is non-line-of-sight so all surfaces are coated with an even thickness including inside and outside corners and blind holes. As it can be observed in Fig. 1a, the coating is compact and, as a consequence, good behaviour of the coating towards mechanical and corrosion solicitations should be expected [1]. The film is formed by columnar, nodular structures (i.e. intercolumnar interstices and small Ni–B nodules), Fig. 1b.

Bath regeneration (i.e. addition of fresh reactive in the bath) induced a new germination phase (represented by a white line on the micrograph) and the structure presents several layers of columns similar in the first step of Ni–B deposition, Fig. 1b. The horizontal lines observed in the deposit correspond to the beginning of a new growth phase after the bath replenishment. The coating thickness calculated from the weight gain, was 30 ± 2 µm.

After heat treatment (Fig. 1c) the structure becomes denser. Some pores in the coatings at the initial deposition stage may result from the evolution of hydrogen during the electroless deposition.

As-deposited Ni–B films are considered to be a mixture of microcrystalline nickel and amorphous Ni–B phases in the as-deposited condition [14,15].

Table 1
Ni–B coating characteristics.

	Roughness parameters [μm]			Wear parameter	Hardness
	Ra	Rq	Rz	TWI	Vickers (hv_{100})
As-plated	0.898 ± 0.063	1.143 ± 0.089	6.318 ± 0.967	28.827 ± 1.244	888 ± 20
Heat treated	0.592 ± 0.082	0.760 ± 0.110	4.069 ± 0.752	13.744 ± 1.950	1302 ± 40

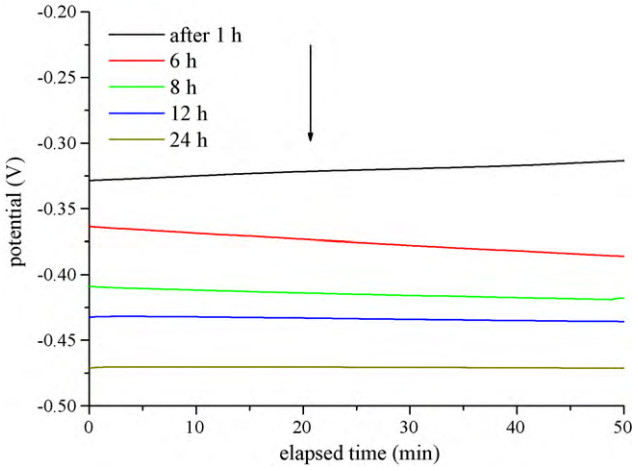

Fig. 2. OCP evolution during 24 h.

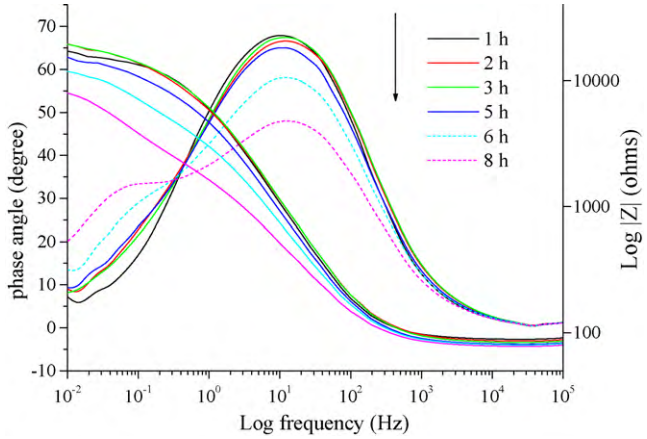

Fig. 3. EIS Bode–Z and phase diagrams of Ni–B coated for several hours.

Heat treatment at 400 °C for 1 h induces crystallization of the Ni–B deposit and the Ni_3B phase appears. The deposit is then totally crystallized into Ni_3B (and possibly some residual Ni) [16]. Heat treatment strongly influences the microstructural and thus the mechanical properties of Ni–B films [17].

3.2. Mechanical tests

The abrasive wear resistance is expressed by the Taber wear index (TWI), which is the weight loss in mg per 1000 wear cycles. The wear index was defined following:

$$\mathrm{TWI} = \frac{(A - B) \times 1000}{C}$$

where A (mg) and B (mg) were the weight for the sample before and after a series of tests of 1000 cycles each. C was the number of rotation cycles which was fixed at 10,000 in this study.

Table 1 summarizes the wear and roughness characteristics. TWI was calculated to evaluate the wear resistance. Smaller wear index represents higher wear resistance. The result proves that the abrasion resistance of the heat treated coating is higher than that of the coatings which are not treated. It appears also that heat treatment tends to make the surface smoother. Heat treatment affects the abrasive wear resistance and the roughness by an important modification of the microstructural properties of Ni–B films [17]. The abrasive wear resistance is increased by hardness increases through grain size refinement, alloying with B and heat treatment.

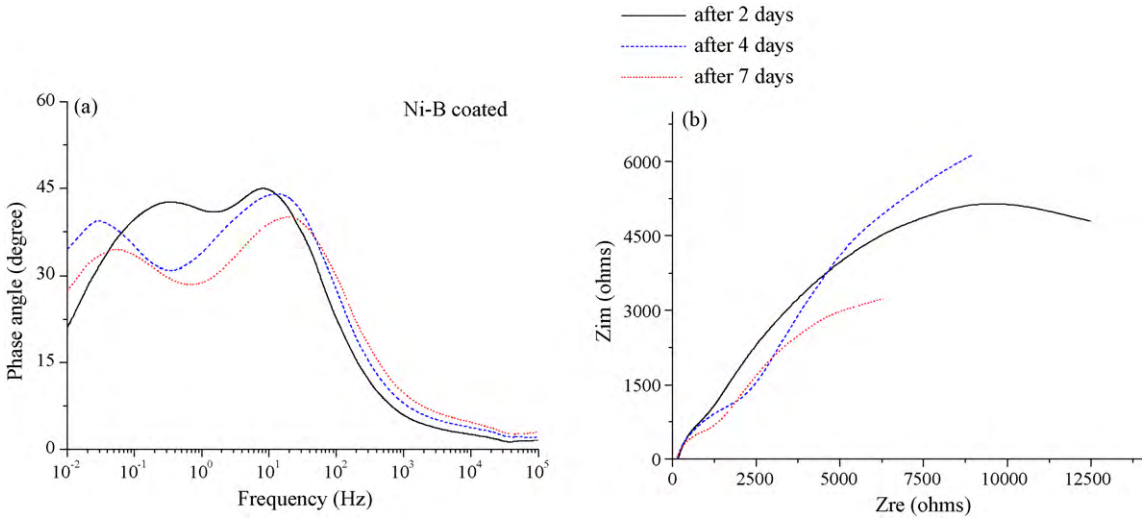

Fig. 4. EIS phase and Nyquist evolutions of Ni–B coated for 7 days.

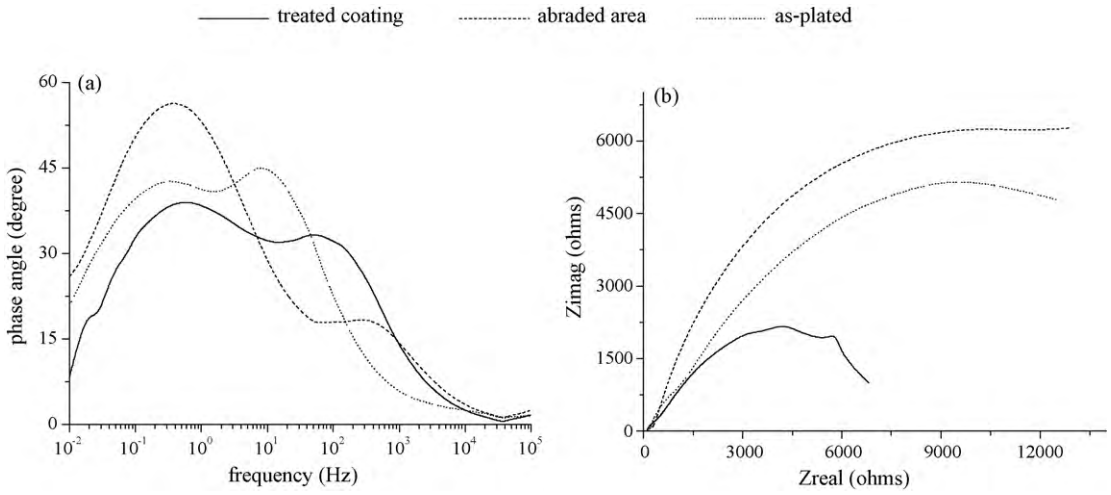

Fig. 5. EIS phase and Nyquist evolutions of as-plated, wearied and heat treated samples after 2 days.

3.3. Corrosion test

3.3.1. Electrochemical impedance spectroscopy

Fig. 2 illustrates the OCP measurement as a function of immersion time in 0.1 M NaCl solution. For each step, it appears that the OCP was stable after 15 min from the beginning of the measurement. However the potential values decrease in time. This behaviour indicates that the corrosion resistance decreases as a function of immersion time.

Fig. 3 shows simultaneously bode phase and *Z* modulus diagram evolutions versus time of immersion for Ni–B coating.

At the beginning (i.e. less than 5 h of immersion), the Bode-modulus diagram presents a single inflection point (Fig. 3). The single loop is related to the coating.

After 6 h of immersion in solution, the phase diagram shows two loops at low and high frequencies. The high frequency response represents the electrical capacitance of the coated film and the low frequency response is related to corrosion phenomena probably due to the penetration of electrolyte through grain boundaries or defects. Contreras et al. [2] explain the part of the phenomena; however these authors did not indicate information about the immersion time.

Fig. 4a shows Bode phase diagram evolutions after 2, 4 and 7 days of immersion in NaCl solution for as-plated coatings. The second time constant is accompanied by a non-negligible decrease of the modulus at low frequency, Fig. 4b. The impedance decrease indicates a loss of protection capacity of the coating, due to electrolyte penetration in defects or grain boundaries [18,19]. Also, boron is not homogeneously distributed throughout the coating, areas of different corrosion potential could be produced on the surface which could explain local attacks of the coating [1].

Fig. 5 compared EIS spectra for as-plated, worn and heat treated sample after 2 days of immersion in 0.1 M NaCl solution. The diameter of the EIS loops is different for each sample and the presence of several inflexion points in the Bode phase diagram confirms that the corrosion process involves more than one time constant [18], Fig. 5a.

Upon heat treatment, the size of the capacitive loop decreases, Fig. 5b. Taking into account the charge transfer resistance values with the loops, it can be noted that the dissolution process is more intense after heat treatment than in the case of as-plated. Heat treatments induce crystallization of the coating [17] that first presents an amorphous-like character and this causes the corrosion resistance of the film to decrease.

The corrosion resistance behaviour can be attributed to the structural modification of the coating: the crystallization that occurs during heat treatment can be accompanied by the formation of defects and grain boundaries that are of lesser importance in as-plated coatings [13,20].

Wear increases significantly surface roughness, induces cracks and finally modifies the coating structure. The decrease in corrosion properties is directly linked to the surface characteristics.

3.3.2. Potentiodynamic polarization curves

Polarization curve of the as-plated Ni–B deposit is shown in Fig. 6. The samples were first immersed into the electrolyte for about 15 min to stabilize the open-circuit potential (OCP). The cathode reaction in the polarization curves corresponds to reduction of dissolved oxygen, and the anodic polarization curve is the most important feature related to the corrosion resistance [21]. The polarization curves of as-plated Ni–B layer showed no passive behaviour of the nickel–boron coating, as is expected of nickel-based alloys. The same phenomenon is observed on curves obtained for heat treated and worn samples. As shown on Fig. 6, Ni–B coating increases significantly the corrosion resistance of the steel. However, the immersion in NaCl solution attacks the grain boundaries and may induce a modification of the deposit structure (such as intercolumnar cracks apparition) by the diffusion phenomena. Consequently the corrosion resistance decreases after immersion in solution (after 19 h of immersion). This was confirmed by impedance test.

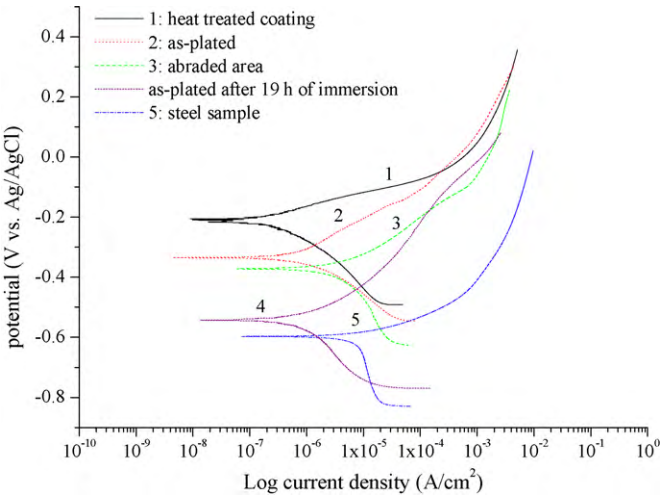

Fig. 6. Potentiodynamic polarization curves.

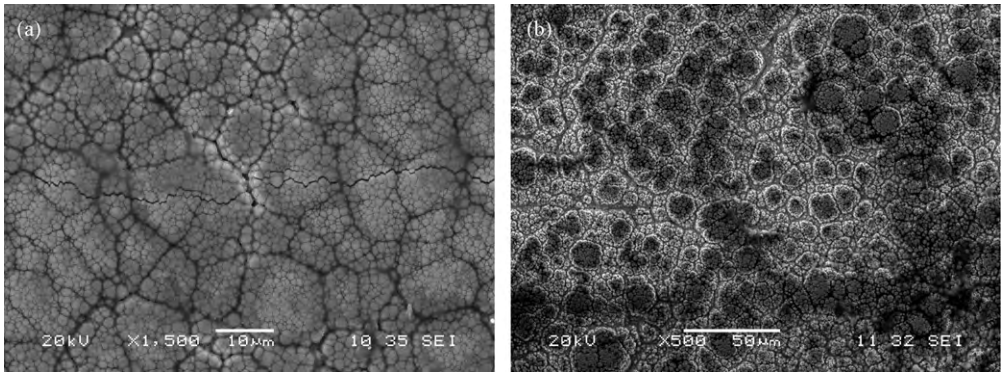

Fig. 7. Morphology of surfaces after EIS tests: (a) after 24 h of immersion; (b) after 21 days of immersion.

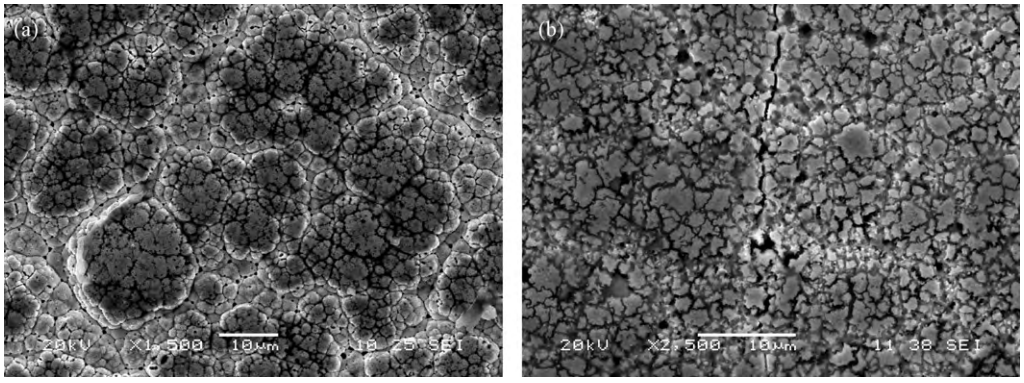

Fig. 8. Morphology of surfaces: (a) after polarization; (b) after 19 h of EIS cycle + polarization test.

3.3.3. Corrosion process

Fig. 7a and b presents respectively SEM micrographs of the surface after 24 h and 21 days of immersion in solution. One notes the presence of localized cracks (Fig. 7a), i.e. that dissolution is preferential at the boundaries of adjacent grains and columns.

Fig. 7b denotes the presence of "black spots" on surface. These could be explained by the important aggressiveness of the chloride ions present in the solution. However the lack of passive behaviour in the polarization curve of the coatings indicates that the presence of chloride cannot imply pitting. This phenomenon can be attributed to galvanic coupling due to composition heterogeneities in the coating [22].

Fig. 8a and b presents respectively the worn surfaces of samples after polarization and after successively 19 h of EIS and polarization corrosion testing.

The surface state of Ni–B deposits is strongly altered after tests: localized corrosion features can be observed. In Fig. 8a the structure is very spongy compared with Fig. 7b (after 21 days) and in the same time attacks are significantly discernible.

The immersion in NaCl solution makes the process more severe, Fig. 8b. Cross section analyze showed that the cracks were limited in depth and do not reach the substrate. Those phenomena could be due to the relatively important deposit thickness (~30 μm).

4. Conclusion

Ni–B coatings are mainly formed by small nodules. SEM of the cross-sectional view of the coatings reveals that the coatings are uniform and the compatibility between the layers is good.

Ni–B coating improves the corrosion resistance of steel sample. The mechanical properties of as-deposited coatings are enhanced by heat treatment. Upon heat treatment, Ni–B coatings crystallize into nickel borides. SEM cross-sectional view of the coatings reveals that the coatings are uniform and the compatibility between the layers is good.

The corrosion resistance evaluation showed that electroless Ni–B coating suffered from severe attacks in 0.1 M NaCl solution in both as-deposited and heat treated coatings.

Observation of corroded coatings after polarization tests and immersion in saline solution showed that the coating's sensitivity to corrosion was linked to the intercolumnar zones, probably because of their lesser density and slightly different chemistry that could lead to the establishment of galvanic coupling between nickel and iron.

Acknowledgements

The authors wish to thank the INISMa (Mons, Belgium) for the SEM analysis.

One of the authors (V. Vitry) wishes to thank the FRIA (Fonds pour la Formation à la Recherche dans l'Industrie et l'Agriculture) for funding.

References

[1] T.S.N. Sankara Narayanan, K. Krishnaveni, S.K. Seshadri, Mater. Chem. Phys. 82 (2003) 771.
[2] A. Contreras, C. León, O. Jimenez, E. Sosa, R. Pérez, Appl. Surf. Sci. 253 (2006) 592.
[3] F. Delaunois, J.P. Pelitjean, P. Lienard, M. Jacob-Duliere, Surf. Coat. Technol. 124 (2000) 201.
[4] M.M. Younan, I.H.M. Aly, M.T. Nageeb, J. Appl. Electrochem. 32 (2002) 439.
[5] R.N. Duncan, T.L. Arney, Plat. Surf. Finish. 71 (1984) 49.
[6] Z. Longfei, L. Shoufu, L. Pengxing, Surf. Coat. Technol. 36 (1988) 455.
[7] R.N. Duncan, T.L. Arney, Plat. Surf. Finish. 76 (1989) 60.
[8] D.J. Flis, Duquette, Corrosion 41 (1985) 700.
[9] G. Salvago, G. Fumagalli, Met. Finish. 85 (1987) 31.

[10] A. Krolikowski, European Federation of Corrosion Publication 2 (1993) 119.
[11] V. Petukhov, M.G. Shcherban, N.E. Skryabina, L.N. Malinina, Prot. Met. 38 (2002) 370.
[12] F. Delaunois, P. Lienard, Surf. Coat. Technol. 160 (2002) 139.
[13] T.S.N. Sankara Narayanan, S.K. Seshadri, J. Alloys Compd. 365 (2004) 197.
[14] W.T. Evans, M. Schlesinger, J. Electrochem. Soc. 141 (1994) 78.
[15] C.T. Dervos, J. Novakovic, P. Vassiliou, Mater. Lett. 58 (2004) 619.
[16] A.-F. Kanta, V. Vitry, F. Delaunois, Mater. Sci. Forum 638–642 (2010) 846.
[17] F. Delaunois, P. Lienard, Surf. Coat. Technol. 160 (2002) 239.
[18] J.N. Balaraju, T.S.N. Sankara Narayanan, S.K. Seshadri, J. Solid State Electrochem. 5 (2001) 334.
[19] F. Vacandio, Y. Massiani, P. Gergaud, O. Thomas, Thin Solid Films 359 (2000) 221.
[20] M. Anik, E. Korpe, E. Sen, Surf. Coat. Technol. 202 (2008) 1718.
[21] C.D. Gu, J.S. Lian, J.G. He, Z.H. Jiang, Q. Jiang, Surf. Coat. Technol. 200 (2006) 5413.
[22] M. Crobu, A. Scorciapino, B. Elsener, A. Rossi, Electrochim. Acta 53 (2008) 3364.